

1986

# Analysis of the Influence of Valve Geometric Parameters on the Effective Flow and Force Areas

T. S. Ferreira

J. Lainor

Follow this and additional works at: <https://docs.lib.purdue.edu/icec>

---

Ferreira, T. S. and Lainor, J., "Analysis of the Influence of Valve Geometric Parameters on the Effective Flow and Force Areas" (1986). *International Compressor Engineering Conference*. Paper 558.  
<https://docs.lib.purdue.edu/icec/558>

This document has been made available through Purdue e-Pubs, a service of the Purdue University Libraries. Please contact [epubs@purdue.edu](mailto:epubs@purdue.edu) for additional information.

Complete proceedings may be acquired in print and on CD-ROM directly from the Ray W. Herrick Laboratories at <https://engineering.purdue.edu/Herrick/Events/orderlit.html>

# ANALYSIS OF THE INFLUENCE OF VALVE GEOMETRIC PARAMETERS ON THE EFFECTIVE FLOW AND FORCE AREAS

Rogério T.S. Ferreira<sup>1</sup> and José L. Driessen<sup>2</sup>

<sup>1</sup>Department of Mechanical Engineering, Federal University of Santa Catarina, 88000 Florianópolis-SC-Brazil, <sup>2</sup>EMBRACO - Empresa Brasileira de Compressores S.A., 89200-Joinville-SC-Brazil

## ABSTRACT

The effective flow and force areas of valves are important parameters for the numerical simulation of reciprocating hermetic compressors, which is a fundamental step in the optimization process.

This work analyzes the effects of the independent variation of different geometric dimensions of hermetic compressor valves on the effective flow and force areas using a circular valve plate, such as valve disc diameter, valve seat step height, valve seat step radius, valve port length, entrance port radius, exit port radius, entrance port conicity and exit port conicity.

The results are presented in dimensionless form using some characteristic parameters. The flow Reynolds number is kept constant when the valve separation is varied.

It is also presented the analysis of the different flow regimes which are encountered when the valve disc is separated from the seat and a detailed description of the experimental setup as well.

## INTRODUCTION

The variation of the thrust force on the reed with the valve lift may lead to vibrations and valve flutter, particularly in connection with a valve spring. This behavior is undesirable in valves design.

Different valve, port and seat geometries affect the effective flow area and the effective force area. Those parameters are needed for the numerical simulation of hermetic compressors and they can also be used to evaluate the expected performance of a compressor valve.



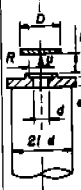
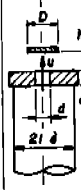
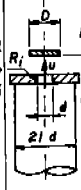
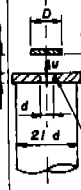
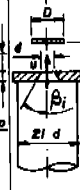

This paper presents the experimental results of the effective

flow and force areas, as defined by Schwerzler & Hamilton <sup>12</sup>, of valves with circular discs considering the variation of different geometrical parameters, as shown in Table I. The results are presented in dimensionless form with respect to the valve lift keeping the flow Reynolds number constant.

The main geometric parameters, whose influence are analyzed are:

- a) Valve disc diameter,  $D$
- b) Valve seat step height,  $H$
- c) Valve seat step radius,  $R$
- d) Valve port length,  $e$
- e) Entrance port radius,  $R_i$
- f) Exit port radius,  $R_o$
- g) Entrance port conicity,  $\beta_i$
- h) Exit port conicity,  $\beta_o$

Table I - Different flow geometries and variable parameters

	(a)	(b)	(c)	(d)	(e)	(f)	(g)	(h)
VARIABLE GEOMETRIC PARAMETER	$D$	$H$	$R$	$e$	$R_i$	$R_o$	$\beta_i$	$\beta_o$
FLOW GEOMETRY								

### FLOW CHARACTERIZATION

For a relatively small distance between the valve disc and the seat, and a sufficiently low Reynolds number, the radial flow is laminar and the pressure drop in the radial direction is due to the predominance of viscous effects. For viscous flow, the radial pressure distribution decreases logarithmically downstream whereas for ideal flow it is predicted to increase radially as shown by Killmann <sup>11</sup>. A laminar flow solution predicting the radial pressure distribution has been obtained by Woolard <sup>1</sup>, Livesey <sup>2</sup>, Jackson & Symmons <sup>5</sup>. The principal methods used, when the inertia terms were included, were the Pohlhausen method to represent the velocity profile and the von Kärman momentum integral method. As pointed out by Bird, Stewart & Lightfoot <sup>6</sup>, the assumption of a fixed velocity profile leads to an inconsistency which may be significant, after Savage <sup>4</sup> and Raal <sup>7</sup>.

With increasing volume flow rate, the Reynolds number at the

inlet may exceed a critical value, so that turbulent flow will exist for some distance downstream of the inlet corner. When the velocity, which decreases with increasing radius, has fallen sufficiently for the local Reynolds number to become subcritical, a reverse transition from turbulent to laminar flow results.

If the volume flow rate is increased still more, the radial flow becomes fully turbulent, and the inertia terms predominate over the viscous terms in determining the pressure distribution. The pressure then rises in the radial direction. In practice, negative pressure gradients are usually found at small radii, changing to positive gradients further out. This makes the valve disc to be attracted to the seat reducing the effective flow area. There appears to have been little theoretical work done on the radial pressure distribution of turbulent flow between valve disc and seat.

As the valve moves away from the seat, the flow will eventually separate near the inlet corner and will then reattach, forming an annular separation bubble. As this distance is increased further, this separation bubble will increase in length until the flow finally fails to reattach, forming a radial wall jet on the valve disc.

The theoretical solution mentioned above are only valid as approximations for the limited case of low Reynolds numbers and a very narrow gap. For higher Reynolds number and a larger gap, the pressure distribution has to be determined numerically. The method used so far, has been the integration of the vorticity transport equation for radial incompressible flow using a finite difference procedure. Hayashi et al.<sup>8</sup> used an iterative relaxation method and obtained solutions for  $Re_d \leq 500$  and  $h/d \leq 0.30$ . Raal<sup>7</sup> obtained the solution in the form of stream function and vorticity distributions from which the velocity and pressure distributions were calculated, for  $Re_d \leq 120$ , where  $d$  is the port diameter.

Raal<sup>7</sup> found that for  $Re_d \leq 24$  there is no separation in spite of the still strongly adverse pressure gradient along the wall. He also determined that the separation point moves upstream with increasing Reynolds number and that the length of the separation bubble increases rapidly with  $Re_d$ .

As indicated by Böswirth<sup>13, 18</sup> and Driessen & Ferreira<sup>14</sup>, Fig. 1 illustrates the pressure distribution on the valve disc for different valve lifts, while the flow rate was kept constant and  $D/d = 3.0$ .

Experimental studies used to substantiate the theoretical solutions are presented in Table II with the main parameters being indicated.

Møller<sup>3</sup> used a nozzle with a sharp edged port and also with a radius of curvature at the port outlet section. He concluded that there was not much difference in the pressure distribution on the valve disc for the sharp or the shaped entry flow boundary.

Tsui et al.<sup>15</sup> studied the flow phenomena of a two-dimensional poppet-type valve using water as the working fluid. The nozzle

used had a valve seat step height  $H/d = 0.148$ . He concluded that the flow regime is divided into two regions: an inner one where the flow can be considered as inviscid and an outer one with turbulent jet flow characteristics. His results indicate that the discharge phenomena can be predicted as a function of the geometry of the valve assembly.

Touber <sup>16</sup> measured the flow and force coefficients for air and R-22 considering different port geometries with sharp and rounded edges at the entrance and exit sections. The specification of the flow Reynolds number is not clear in each experiment. These measurements were used as coefficients to a semi-empirical mathematical compressor model.

All the other experimental studies listed in Table II used sharp edged ports and plane circular valves.

### BASIC EQUATIONS

The method used for the experimental determination of the effective flow area in steady state is proposed by Soedel <sup>17</sup> and it is based on the measurement of the mass flow rate through the valve system being tested, the pressure drop across the valve and the density of the gas upstream of the valve.

The mass flow rate  $\dot{m}$  through the orifice flowmeter built according to ASME recommendations <sup>19</sup> is calculated by Eq.(1).

$$\dot{m} = K Y A \sqrt{\rho h_w} \quad (1)$$

where  $K$  is the orifice flow coefficient,  $Y$  is the expansion coefficient,  $A$  is the orifice area,  $\rho$  is the gas density upstream the orifice meter and  $h_w$  is the pressure drop across the meter. The discharge coefficient  $K$  is a function of the local Reynolds number for fixed diameters ratio (orifice diameter/pipe diameter) and  $Y$  depends on the pressure drop across the orifice meter and the absolute pressure ahead the flowmeter.

The mass flow rate across the valve assembly is given, for a subsonic flow by

$$\dot{m} = p_m A_{ep} \sqrt{\frac{2k}{(k-1)R T_m}} \sqrt{r^{2/k} - r^{(k+1)/k}} \quad (2)$$

Where  $p_m$  and  $T_m$  are the absolute pressure and absolute temperature upstream of the valve assembly,  $A_{ep}$  is the equivalent flow area,  $R$  is the gas constant,  $k$  is the gas relation of specific heats and  $r$  is the pressure relation downstream and upstream of the valve assembly.

Combining Eq. (1) and (2), one can get the equivalent flow area

$$A_{ep} = \frac{K Y A \sqrt{\rho h_w} / p_m}{\sqrt{\frac{2k}{(k-1)R T_m}} \sqrt{r^{2/k} - r^{(k+1)/k}}} \quad (3)$$

Table II - Experimental studies available for comparison with theoretical predictions

Author	Year	Fluid	Re <sub>d</sub> Range	D/d	h/d	p(r)	Thrust Force
Moller (3)	1963	Air	1,7 x 10 <sup>5</sup> 4,3 x 10 <sup>5</sup>	4 and 6	<0,667	Yes	No
Takenaka et al (10)	1964	Water	4,9 x 10 <sup>3</sup> 6,8 x 10 <sup>4</sup>	1,5; 2,5 and 3,0	<0,25	No	Yes
Jackson et al (5)	1965	Air	8,9 x 10 <sup>3</sup> 4,7 x 10 <sup>4</sup>	48	<0,256	Yes	No
Tsui et al (15)	1972	Water	-	1,77	<0,30	Yes	Yes
Hayashi et al (8)	1975	Oil	50-900	3 and 6	<0,20	No	Yes
Touber (16)	1976	Air,R-22	2 x 10 <sup>3</sup> 2 x 10 <sup>4</sup>	1,33	<0,10	No	Yes
Wark & Foss (9)	1984	Air	1 x 10 <sup>3</sup> 7 x 10 <sup>3</sup>	4; 5,33 8 and 24	<0,56	No	Yes

As the valve assembly is located at the end of the pipeline, the pressure ahead of the valve is the sum of the atmospheric pressure and the pressure drop across the valve.

The effective force area is determined by the measurement of the thrust force  $F_{ex}$  on the reed and the pressure difference across the valve assembly,  $\Delta p_v$ .

$$A_{ef} = \frac{F_{ex}}{\Delta p_v} \quad (4)$$

#### EXPERIMENTAL SETUP

The experimental setup used to determine the effective flow and force areas is shown in Fig. 2.

The pressure drop across the orifice flowmeter is measured with an inductive differential pressure transducer HBM 0.01 bar, and the amplifier bridge HBM KWS/GE-5. The pressure ahead of the orifice meter and ahead of the valve assembly are measured with U manometers using water or mercury as working fluids. The temperature ahead of the valve assembly did not show great difference with respect to the ambient temperature and was evaluated by a # 20 AWG copper - constantan thermocouple.

The thrust force on the valve disc was evaluated with a parallel spring dynamometer using two inductive proximity transducers HBM TR 20 and the amplifier bridge HBM KWS/GE-5. The maximum displacement of the dynamometer was 20  $\mu\text{m}$  for a thrust force 0.1 N. The working fluid for the test is air supplied by an air compressor and a reservoir with maximum pressure of 11 bar.

To obtain the required flow and force data, the circular valve reed is set for a certain height. Pressure regulators in the gas supply line are adjusted to provide enough flow rate to the test section, and then the variables are read. For each reed lift from the seat, about 8 readings were performed in order to eliminate the Reynolds number dependence on the effective flow and force areas.

The air flow rate was kept low in order to avoid the compressibility effects and to get the same range of equivalent Reynolds number in all sets of data.

The air flow was characterized by an equivalent Reynolds number, given by Eq. (5)

$$Re_{eq} = \frac{\dot{m} d}{A_{ep} \mu} \quad (5)$$

where  $d$  is the smallest port diameter and  $\mu$  is the air absolute viscosity at the test temperature.

The typical equivalent Reynolds number used for comparing the results were 6,000 , 10,500 and 15,000.

## EXPERIMENTAL RESULTS

The experimental results of effective flow and force areas are presented in Figs. 3 to 18 for all the cases shown in Table I.

The effective flow and force areas are made dimensionless by using the port area ( $A_1$ ) as a parameter. The port diameter ( $d$ ) was used to convert the valve disc separation from the seat into dimensionless form.

Each geometric parameter of the seat, port and valve disc was varied independently in each case, keeping all the others constant.

The equivalent Reynolds number in all cases shown in Figs. 3 to 18 is 10,500. The case  $D/d = 3.0$ , sharp edged port,  $e/d = 0.931$ ,  $H/d = 0.0$  is shown in all Figures and it serves as comparison for the analysis of geometric influence.

The main characteristics introduced by each geometric parameter is listed below:

- a) The plate valve diameter has low influence on the effective flow area but it makes the undesirable negative region of the effective force area to grow when the plate diameter is increased. For  $h/d = 0$  the effective force area is 1.0 for sharp edged ports.
- b) The valve seat step height produces a reduction on the effective flow area but it considerably reduces the negative region of the effective force area. This is related to the reduction of the annular bubble flow separation on the seat.
- c) The valve port length has a peculiar influence on the effective flow area. When this length is low, the flow contraction at the port entrance makes the reattachment to happen in the valve seat away from the port length resulting in a reduction of the effective flow area.
- d) The entrance port radius and the entrance port conicity show similar effects on the effective flow and force areas. The tendency is not very clear yet.
- e) The exit port radius and the exit port conicity tend to increase the effective flow area in the proportional region showing an overshoot for  $h/d \approx 0.2$ . This happens because the smallest port cross section area was used as a parameter and the flow is more easily oriented towards the seat.

A typical equivalent Reynolds number dependence is shown in Figs. 19 and 20 for  $D/d = 3.0$ ,  $e/D = 0.931$  and sharp edged port. The effective force area presents a slightly dependence for small equivalent Reynolds number and small valve disc separation from the seat.

## CONCLUSIONS

The method used for the determination of the effective flow and force areas showed to be adequate for any type of valve assembly where those parameters are important.

The experimental results can be used as a guide for the understanding of the flow behavior throughout the valve and also



as a basis for the analysis of more complex valve geometries.

For hermetic compressors, the negative effective force areas are undesirable as the reed tends to return towards the seat reducing the effective flow area. From the valve assembly standpoint it would be recommended small valve disc diameter, small valve seat step height, small valve seat step radius, valve port radius on the order of port diameter, zero entrance port radius or zero entrance port conicity and large exit port radius or large exit port conicity.

#### REFERENCES

- [1] Woolard, H.W., A Theoretical Analysis of the Viscous Flow in a Narrowly Spaced Radial Diffuser, J. Appl. Mech, Vol. 24, Trans. ASME, Vol. 79, 1957, pp. 9-15.
- [2] Livesey, J.L., Inertia Effects in Viscous Flows, Int. J. Mech. Sci., Vol I, 1960, pp. 84-88.
- [3] Moller, P.S., Radial Flow Without Swirl between Parallel Discs, Aero. Quart., Vol. 14, 1963, pp. 163-186.
- [4] Savage, S.B., Laminar Radial Flow between Parallel Plates, J. Appl. Mech., Vol. 31, 1964, pp. 594-596.
- [5] Jackson, J.D.; Symmons, G.R., An Investigation of Laminar Radial Flow between Two Parallel Discs, Appl. Sci. Res. Section A, Vol. 15, 1965, pp. 59-75.
- [6] Bird, R.B.; Stewart, W.E.; Lightfoot, E.N., Transport Phenomena, John Wiley, 1960.
- [7] Raal, J.D., Radial Source Flow between Parallel Disks, J. Fluid Mech., Vol. 85, 3, 1978, pp.401-416.
- [8] Hayashi, S.; Matsui, T.; Ito, T., Study of Flow and Thrust in Nozzle - Flapper Valves, J. Fluids Eng., Vol. 97, 1975, pp. 39-50.
- [9] Wark, C.E.; Foss, J.F., Forces Caused by the Radial Outflow between Parallel Disks, J. Fluids Eng., Vol. 106, 1984, pp. 292-297.
- [10] Takenaka, T.; Yamane, T.; Iwamizu, T., Thrust of the Disc Valves, Bull. JSME, Vol. 7, N<sup>o</sup> 27, 1964, pp. 558-566.
- [11] Killmann, I.G., Aerodynamic Forces Acting on Valve Discs, Purdue Compressors Technology Conf., 1972, pp. 407-414.
- [12] Schwerzler, D.D.; Hamilton, J.F., An Analytical Method for Determining Effective Flow and Force Areas for Refrigeration Compressor Valving Systems, Purdue Compressors Technology Conf., 1972, pp. 30-36.
- [13] Boswirth, L., Private Communication, 1985.
- [14] Driessen, J.L.; Ferreira, R.T.S., Influência das Dimensões Geométricas das Válvulas no Desempenho de Compressores Herméticos Alternativos, VIII COBEM, pp. 237-239 (in Portuguese).

- |15| Tsui, C.Y.; Oliver, C.C.; Cohen, R., Discharge Phenomena of a Two-Dimensional Poppet-Type Valve, Purdue Compressors Technology Conf.; 1972, pp. 212-220.
- |16| Touber, S., A Contribution to the Improvement of Compressor Valve Design, WTHD 84, 1976.
- |17| Soedel, W., Introduction to Computer Simulation of Positive Displacement Type Compressors, R.W. Herrick Laboratories, 1972.
- |18| Böswirth, L., Theoretical and Experimental Study on Flow in Valve Channels, Part I and II, Purdue Compressors Technology Conf., 1982, pp. 38-53.
- |19| Bean, H.S., Fluid Meters - Their Theory and Application, 6<sup>th</sup> Ed., The American Society of Mechanical Engineers, 1971.

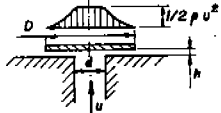
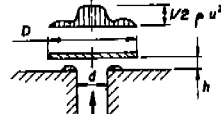
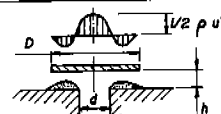
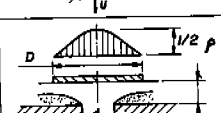

VALVE LIFT	PRESSURE DISTRIBUTION ON VALVE DISC	FLOW CHARACTERIZATION
$h/d < 0.02$		LAMINAR FLOW
$0.02 < h/d < 0.05$		SMALL ANNULAR BUBBLE SEPARATION
$0.05 < h/d < 0.5$		LARGE ANNULAR BUBBLE SEPARATION
$0.5 < h/d < 1.0$		COMPLETE SEPARATION 90° DEFLECTION
$h/d > 1.0$		COMPLETE SEPARATION < 90° DEFLECTION

FIG.1-PRESSURE DISTRIBUTION ON VALVE DISC FOR  $D/d=3.0$  AND CONSTANT FLOW RATE.

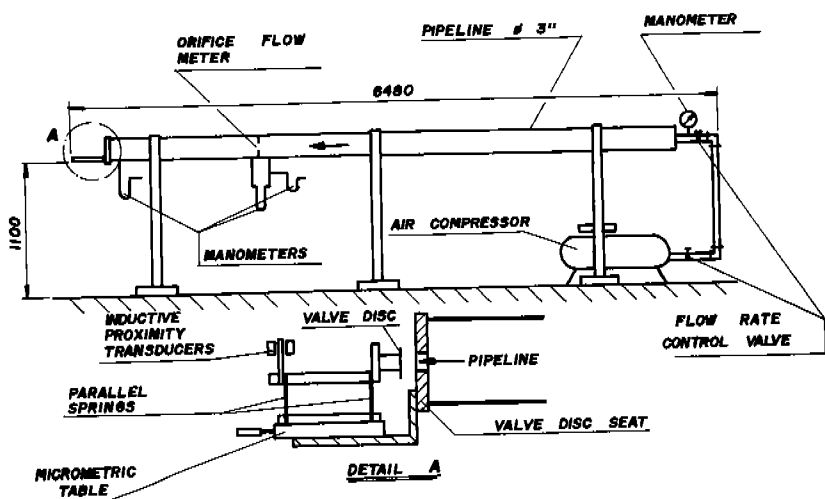


FIG.2- EXPERIMENTAL SETUP.

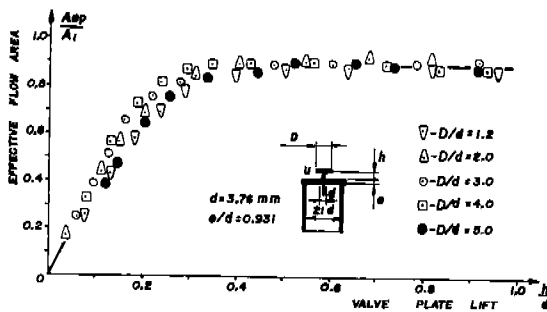


FIG. 3 - INFLUENCE OF VALVE PLATE DIAMETER ON THE EFFECTIVE FLOW AREA

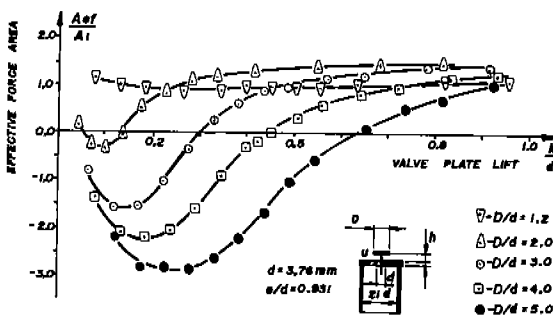


FIG. 4 - INFLUENCE OF VALVE PLATE DIAMETER ON THE EFFECTIVE FORCE AREA

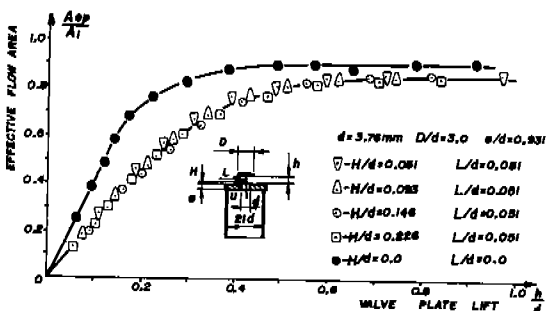


FIG. 5 - INFLUENCE OF VALVE SEAT STEP HEIGHT ON THE EFFECTIVE FLOW AREA

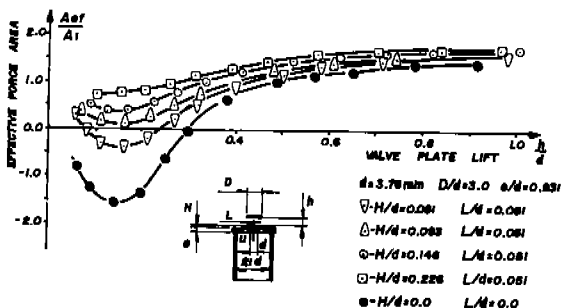
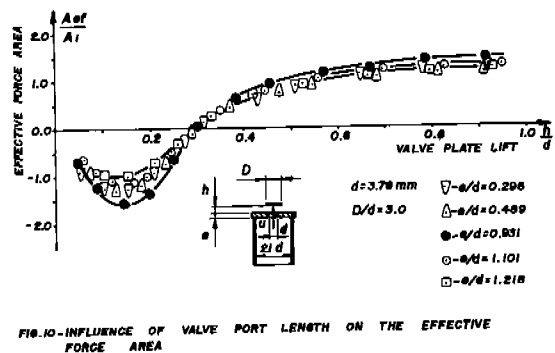
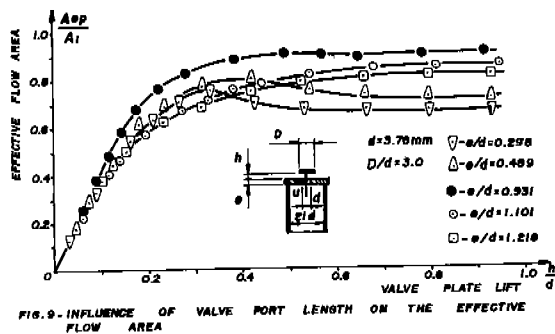
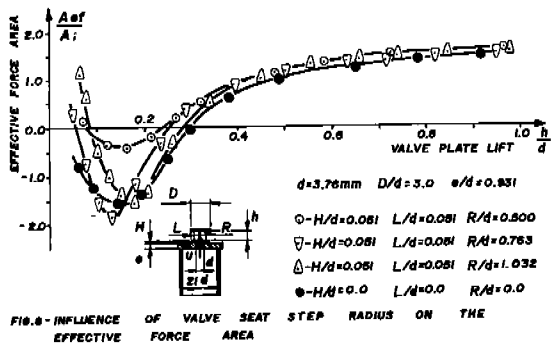
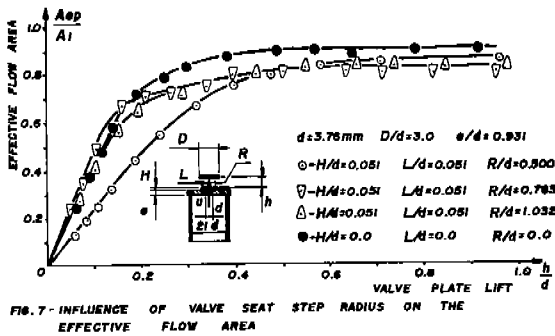


FIG. 6 - INFLUENCE OF VALVE SEAT STEP HEIGHT ON THE EFFECTIVE FORCE AREA



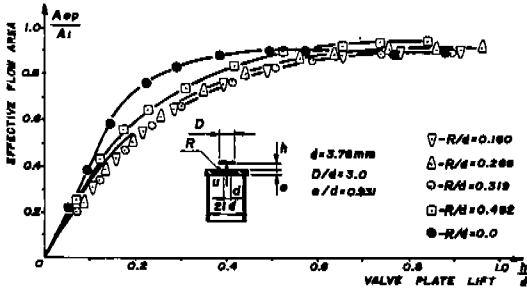


FIG.11-INFLUENCE OF ENTRANCE PORT RADIUS ON THE EFFECTIVE FLOW AREA

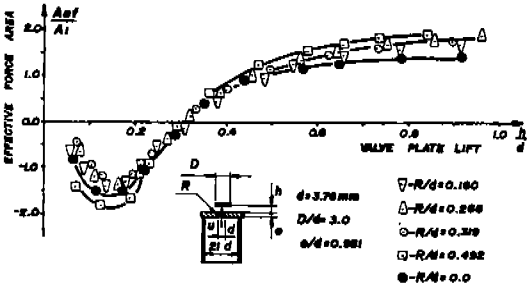


FIG.12-INFLUENCE OF ENTRANCE PORT RADIUS ON THE EFFECTIVE FORCE AREA

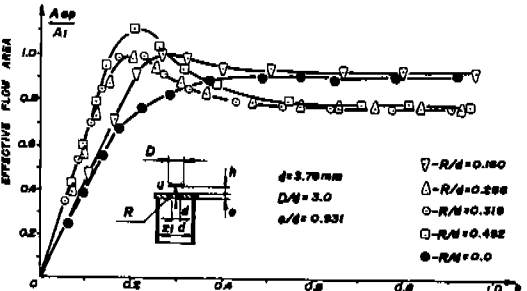


FIG.13-INFLUENCE OF EXIT PORT RADIUS ON THE EFFECTIVE FLOW AREA

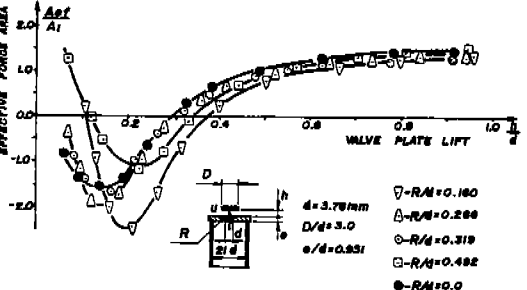


FIG.14-INFLUENCE OF EXIT PORT RADIUS ON THE EFFECTIVE FORCE AREA

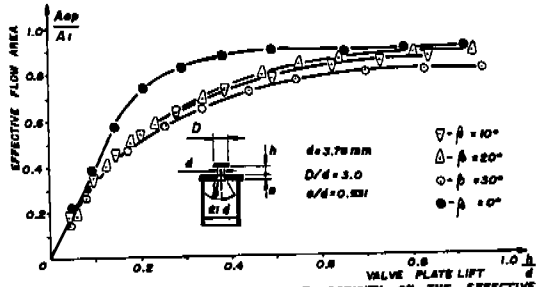


FIG. 17—INFLUENCE OF ENTRANCE PORT CONGRUITY ON THE EFFECTIVE FLOW AREA

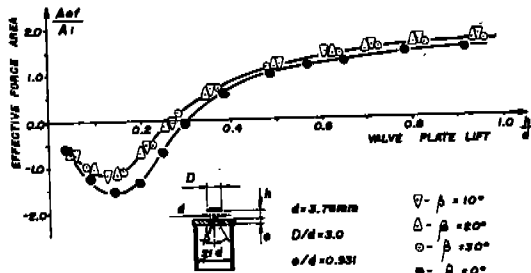


FIG. 18—INFLUENCE OF ENTRANCE PORT CONGRUITY ON THE EFFECTIVE FORCE AREA

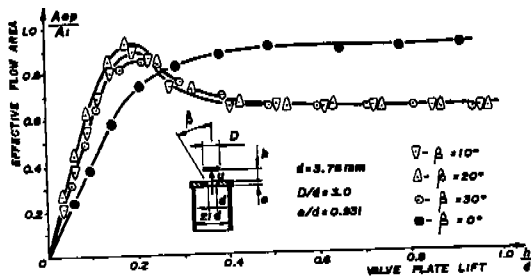


FIG. 17—INFLUENCE OF EXIT PORT CONGRUITY ON THE EFFECTIVE FLOW AREA

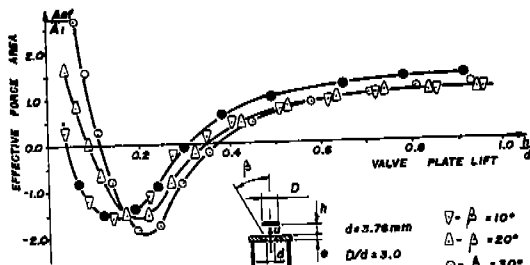


FIG. 18—INFLUENCE OF EXIT PORT CONGRUITY ON THE EFFECTIVE FORCE AREA

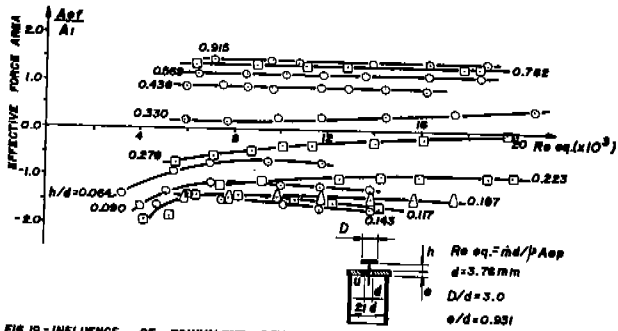


FIG. 19 - INFLUENCE OF EQUIVALENT REYNOLDS NUMBER ON THE EFFECTIVE FORCE AREA

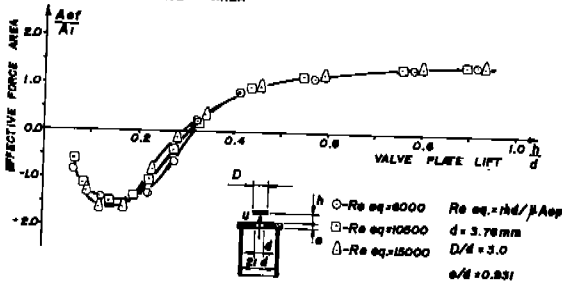


FIG. 20 - INFLUENCE OF EQUIVALENT REYNOLDS NUMBER ON THE EFFECTIVE FORCE AREA